


## Article

# Anti-Corrosion Behavior of Olmesartan for Soft-Cast Steel in 1 mol dm<sup>−3</sup> HCl

B. M. Praveen <sup>1</sup>, A. Alhadhrami <sup>2</sup>, B. M. Prasanna <sup>3,\*</sup> , Narayana Hebbar <sup>4</sup> and Radhakrishna Prabhu <sup>5</sup>

<sup>1</sup> Department of Chemistry, College of Engineering & Technology, Srinivas University, Mukka, Mangalore 574146, India; researchdirector@srinivasuniversity.edu.in

<sup>2</sup> Department of Chemistry, College of Science, Taif University, P.O. Box 11099, Taif 21944, Saudi Arabia; a.babtin@tu.edu.sa

<sup>3</sup> Department of Chemistry, Jain Institute Technology, Davanagere 577003, India

<sup>4</sup> Department of Chemistry, Sri Darmasthala Manjunatheshwara College (Autonomous), Ujire 574240, India; dr.nahebbbar@sdmcyjire.in

<sup>5</sup> School of Engineering, Robert Gordon University, Aberdeen AB10 1FR, UK; r.prabhu@rgu.ac.uk

\* Correspondence: drbmprasanna@jitd.in

**Abstract:** This study discusses the effects of temperature on corrosion inhibition for soft-cast steel by the pharmaceutically active drug olmesartan in 1 mol dm<sup>−3</sup> HCl. The sufficient number of electron-rich elements and non-bonding  $\pi$  electrons in its structure favored a good capability for coating onto the electron-deficient steel surfaces. Theoretical and electrochemical measurements were carried out at the temperature region of 303 K to 333 K. Therefore, the experiment suggests that the inhibition efficiency of olmesartan increases with its increasing concentrations due to the adsorption. Additionally, even at a higher temperature of 333 K, the inhibitor molecules attain their stability towards corrosion resistance of steel surfaces. The adsorption of inhibitors on steel surfaces is spontaneously found to include the mixture of physisorption and chemisorption, and it obeys Temkin's adsorption isotherm model. Theoretical and computational considerations were made using quantum chemical parameters and molecular dynamics simulations, which confirmed that the olmesartan has a suitable corrosion inhibitive capability intended for soft-cast steel in 1 mol dm<sup>−3</sup> HCl. Additionally, scanning electron microscopic measurement was used to obtain a visual idea of the inhibitive action of the inhibitor attained by forming an adsorbed protective layer onto the steel surfaces. The minute concentration of olmesartan of about 10–50 ppm shows high inhibition efficiency of ~80%, even at elevated temperatures.

**Keywords:** soft-cast steel; electrochemical; SEM; adsorption; molecular dynamic simulation



**Citation:** Praveen, B.M.; Alhadhrami, A.; Prasanna, B.M.; Hebbar, N.; Prabhu, R. Anti-Corrosion Behavior of Olmesartan for Soft-Cast Steel in 1 mol dm<sup>−3</sup> HCl. *Coatings* **2021**, *11*, 965. <https://doi.org/10.3390/coatings11080965>

Academic Editor: Tao-Hsing Chen

Received: 10 July 2021

Accepted: 10 August 2021

Published: 13 August 2021

**Publisher's Note:** MDPI stays neutral with regard to jurisdictional claims in published maps and institutional affiliations.



**Copyright:** © 2021 by the authors. Licensee MDPI, Basel, Switzerland. This article is an open access article distributed under the terms and conditions of the Creative Commons Attribution (CC BY) license (<https://creativecommons.org/licenses/by/4.0/>).

## 1. Introduction

Soft cast steel is one of the most important iron alloys with a lower carbon content (i.e., carbon content less than 0.15%). These have industrial, automobile, and construction applications because of their superior thermal and mechanical stability. Hence, soft-cast steel is cast off for many practices viz., acid pickling, descaling, oil well acidifying, petroleum refineries, etc. [1,2]. Under these conditions, steel surface exposure with aggressive media leads to corrosion. Hence, various methods are to be adopted, such as anodization, cathodic protection, coatings, and corrosion inhibitors, for metal protection by corrosion. Among those different practices of protecting the metal, the use of corrosion inhibitors is the most appropriate, experimentally acceptable, and cost-effective technique [3].

Corrosion inhibitors are organic heterocyclic compounds that contain electron-rich N, S, O, and non-bonding  $\pi$  electrons present in the heterocyclic ring system of its structure. Through these, the inhibitor molecules are coated onto the electron-deficient metal surfaces [4]. Similarly, various physio-chemical properties of an inhibitor play an important role in determining adsorption capability onto steel surfaces [5].

Earlier research has already proven that many organic heterocyclic compounds act as corrosion inhibitors, which have shown good inhibition efficiency for various metals such as steel, aluminum, zinc, and copper in various aggressive media. In this context, a few commercially available drug intermediates, such as clotrimazole [6], Rizatriptan [7] Telmisartan [8], Seroquel [9], sulfamethoxazole [10], Praziquantel [11], Ketosulfide [12], Aspirin [13], Anthranilic Acid [14], and few novel synthesized molecules such as tert-butyl 4-[(4-methyl phenyl) carbonyl] piperazine-1-carboxylate [15], 4,5,6,7-Tetrahydro-1,3-benzothiazole [16], 1,3-bis(1-Phenylethyl) Urea [17] N1-(3-Methylphenyl) Piperidine-1,4-Dicarboxamide [18] etc., show good corrosion inhibition efficiency for metal surfaces in aggressive acidic media. However, a large number of studied corrosion inhibitors effectively inhibit steel corrosion in the current scenario, showing promising results. However, reported corrosion inhibitors may be toxic, less stable at a higher temperature, experimentally time-consuming. However, in our study, this selected olmesartan was investigated theoretically by quantum chemical calculations. This primary investigation was done by using it without any experimental work and within a short period. Therefore, this quantum method plays a vital role in showing whether or not the selected organic heterocyclic compound acts as a corrosion inhibitor by using its molecular orbits. In addition, the molecular dynamic simulation study strengthens quantum results. Later, these theoretical predictions were confirmed by conducting real corrosion experiments [19].

The quantum and MD simulation method is a promising theoretical method for obtaining information about a system at the molecular level. Therefore, the basic principle of quantum and MD simulation, as well as methods, parameters, and applications in corrosion inhibition, are discussed in this study. This research also looks at how to choose parameters like the energy gap, dipole moment, force field, time step, and ensemble when running a quantum and MD simulation for corrosion studies, which, to our knowledge, has only been discussed in a few papers. The scope of this MD calculation is rare in recent studies, particularly those involving ferrous metal corrosion inhibition using corrosion inhibitors in acidic solutions [20].

Therefore, it takes less time to decide the feasibility of an organic compound that acts as an effective corrosion inhibitor for soft-cast steel in  $1 \text{ mol dm}^{-3}$  HCl. Therefore, the corrosion experiments were done by electrochemical techniques such as potentiodynamic polarization and impedance spectroscopy. These electrochemical methods give more accuracy and higher sensitivity and are cheap and user-friendly for conducting experiments compared to other methods [21]. The scanning electron microscopic measurements provide a visual representation of the process of establishing a protective barrier on metal surfaces from the bulk of the solution [22]. Therefore, olmesartan has more nitrogen and oxygen with  $\pi$ -electrons in heterocyclic rings, allowing it to serve as a suitable corrosion inhibitor for soft-cast steel in  $1 \text{ mol dm}^{-3}$  HCl. The major motivation to select this olmesartan as a corrosion inhibitor for steel is that a minute concentration is used to get stable coating onto the metal surfaces in 1 M HCl, leading to control of the corrosion.

## 2. Experimental Section

### 2.1. Soft Cast Steel

Soft cast steel with the dimension of  $6 \times 1 \times 0.05 \text{ cm}^3$  was procured commercially for this investigation. The steel strip was clean and dry, then mechanically abraded by SiC papers (grade no 100 up to 2500) until we achieved good finishing, and we used it for all corrosion inhibition experiments. The elementary composition of soft-cast steel is listed in the following Table 1.

**Table 1.** Elemental composition of soft-cast steel used for corrosion experiments.

Elements	C	Mn	P	S	(Fe)
(%)	0.41	0.029	0.031	0.04	Rest

## 2.2. Inhibitor

The olmesartan is an imidazole derivative drug, which is procured commercially, was selected as a corrosion inhibitor, and its molecular structure is shown in Figure 1. It is colorless crystalline in nature, which is soluble in HCl. The standardized  $1 \text{ mol dm}^{-3}$  HCl solution was prepared with triple-distilled water. Therefore, the various increasing concentrations from 10 to 50 ppm of olmesartan were dissolved in  $1 \text{ mol dm}^{-3}$  HCl as the inhibited solution.

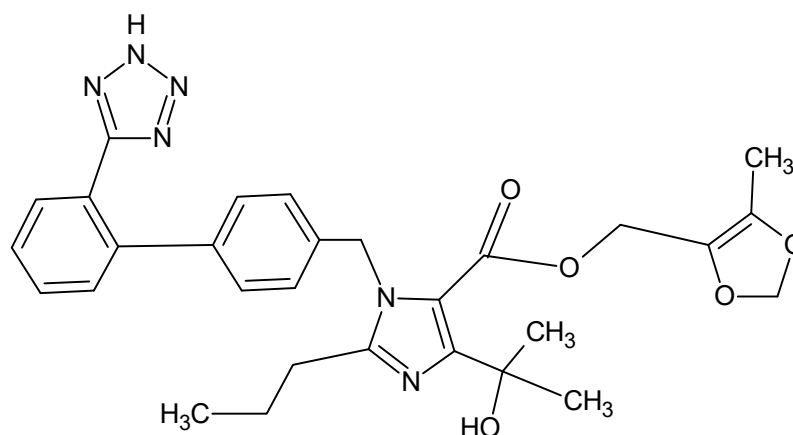


**Figure 1.** Molecular structure of olmesartan.

## 2.3. Quantum Studies

The inhibition effect of any organic heterocyclic molecule is primarily estimated theoretically by quantum chemical calculations. Quantum tests were conducted using Hyperchem Technical Software 8.0 with complete olmesartan molecule geometry. With a 6-31 G\*\* basis collection, DFT raised the optimized molecular structure of olmesartan. To make calculations simple and accurate, the Polak–Riebert algorithm was used.

## 2.4. Molecular Dynamics Simulations

The Hypercom 8.0 software was used to conduct the current study of molecular dynamics (MD) simulations. For the simulation tests, the Fe (110) surface was chosen. The interaction of the inhibitor molecule with the metal surface was studied in a simulation box with boundary conditions (39.47 39.47 77.230 Å). To obtain accurate data, the experiments used ten layers of iron atoms. As a result, the simulation box was used to build the iron, solution, and vascular layers. The MD simulation box was created to represent atomic simulation experiments (COMPASS) with a molecular potential optimized for the condensed phase. These MD simulations were carried out at both 0.0010 and 1 ps in time.

## 2.5. Electrochemical Techniques

Electrochemical techniques were used for the corrosion-inhibitive capability of olmesartan in  $1 \text{ mol dm}^{-3}$  HCl at a high-temperatures ranging from 303 K to 333 K. Electrochemical workstation Ivium compact state e10800 with a three-electrode assembly connection was used for all electrochemical measurements for corrosion experiments. A working electrode (soft-cast steel strip), a counter electrode (platinum wire), and a reference electrode (saturated calomel electrode) made up the three-electrode system. In the electrochemical polarization measurements, in the given range of potential by the scan rate of  $1 \text{ mV s}^{-1}$ , a potentiodynamic Tafel plot of potential against the current was reported. For electrochemical impedance spectroscopy (EIS) measurements, spectra were plotted with AC signals with an amplitude of 0.01 V/s for open circuit potential at a frequency ranging from 10 kHz to 0.1 Hz.

## 2.6. Scanning Electron Microscopy (SEM) Measurement

The 1 cm<sup>2</sup> soft-cast steel strips were mechanically rubbed with emery paper and degreased with acetone, accompanied by triple-distilled water. Two smooth-surfaced strips were immersed in 1 M HCl alone and then with the addition of 50 ppm concentration for 6 h. After that, both the steel strips were taken out and washed with acetone, and then distilled water. Steel strips were dried at room temperature and subjected to SEM analysis using a scanning electron microscope.

## 3. Result and Discussions

### 3.1. Quantum Calculations

Quantum calculations are a powerful technique used to decide the feasible factors of organic compounds as suitable corrosion inhibitors by using molecular orbitals. This study was conducted using the electron density distribution for various geometries of molecules. Figure 2 illustrates the optimized structure of the olmesartan molecule. The frontier molecular orbitals (FMOs), such as the highest occupied molecular orbitals (HOMOs) and the lowest unoccupied molecular orbitals (LUMOs), are shown in Figures 3 and 4 respectively. These FMOs can evaluate the reactivity of chemical compounds.

The energy states of HOMO ( $E_{\text{HOMO}}$ ) and LUMO ( $E_{\text{LUMO}}$ ) values are vital to study the chemical interaction.  $E_{\text{HOMO}}$  indicates electron donation capacity. Higher  $E_{\text{HOMO}}$  values suggest that the inhibitor has a greater ability to donate electrons and, hence, higher inhibition efficiency. Therefore, the value of  $E_{\text{LUMO}}$  is the capacity of the molecule, which accepts electrons from the metal. The lesser its value, the higher its ability to accept electrons will be [23]. The results found from this study suggest that the  $E_{\text{HOMO}}$  value is  $-8.182$  and the  $E_{\text{LUMO}}$  value is  $-1.156$ . The higher energy values of  $E_{\text{HOMO}}$  and lesser values of  $E_{\text{LUMO}}$  strongly imply that olmesartan is an excellent inhibitor. Therefore, the inhibitive efficiency of olmesartan is determined by the energy gap ( $\Delta E$ ) between HOMO and LUMO. The lower value of  $\Delta E$  indicates maximum adsorption chances of the inhibitor [24]. Higher polarisation with more chemical reactivity and lower kinetic stability is obtained when the energy gap is small. In our studies, the  $\Delta E$  value is 7.026, and it is relatively comparable with our earlier results. Mahendra Yadav et al. investigated the corrosion inhibition of three Benzimidazole derivatives and found that  $\Delta E$  values are 8.059 eV, 7.963 eV, and 7.947 eV for Inh 1, Inh 2, and Inh 3, respectively [25]. J Zhang et al. studied the corrosion-inhibitive characteristics for imidazoline phosphate and discovered an  $\Delta E$  value of 8.83 eV with a 95% inhibition efficiency [26]. In a study of a few organic compounds, Nataraj et al. found  $\Delta E$  values of 8.13 eV, 6.56 eV, 5.47 eV, and 5.47 eV for the three inhibitors such as HYD, TAD, and TRD, respectively [27]. HOMO and LUMO both refer to the ionization potential and electron affinity of the molecule. In general, the capacity or potentiality of a molecule can be defined in terms of some parameters. The vital parameters of the molecule decide the inhibitive capability such as ionization potential ( $I$ ), electron affinity ( $A$ ), electronegativity ( $\chi$ ), global hardness ( $\eta$ ), and global softness ( $\sigma$ ) were calculated by HOMO and LUMO energies, and the mathematical expressions used to calculate them are as follows. Table 2 lists the calculated quantum chemical parameters.

$$A = -E_{\text{LUMO}} \quad (1)$$

$$I = -E_{\text{HOMO}} \quad (2)$$

$$\chi = \frac{I + A}{2} \quad (3)$$

$$\alpha = -\frac{I + A}{2} \quad (4)$$

$$\eta = \frac{I - A}{2} \quad (5)$$

$$\sigma = -\frac{I - A}{2} \quad (6)$$

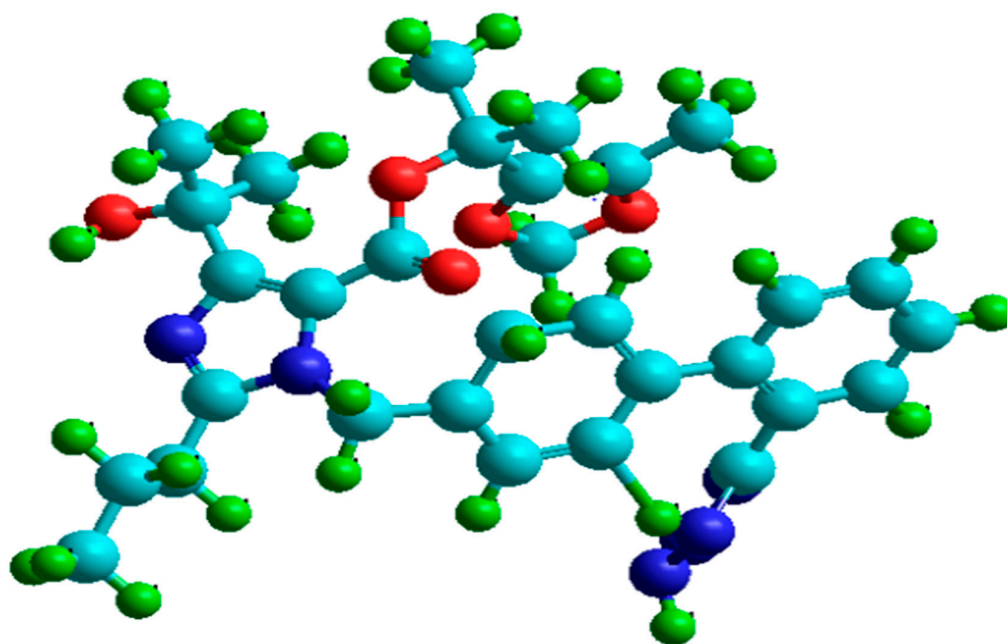
**Table 2.** Quantum chemical parameters of olmesartan molecules.

Sl. No.	Quantum Chemical Parameters	Olmesartan
1	Molecular Formula	C <sub>29</sub> H <sub>32</sub> N <sub>6</sub> O <sub>5</sub>
2	Molecular Weight	544.60 amu
3	Total Energy	−244.84 a.u
4	E <sub>HOMO</sub>	−8.182 eV
5	E <sub>LUMO</sub>	−1.156 eV
6	$\Delta E = E_{LUMO} - E_{HOMO}$ (eV)	7.026 eV
7	Dipole Moment ( $\mu$ )	7.83 Debye
8	Ionization Potential, ( <i>I</i> )	8.182
9	Electron Affinity ( <i>A</i> )	1.156
10	Electronegativity ( $\chi$ )	4.669
11	Global hardness ( $\eta$ )	3.513
12	Global Softness ( $\sigma$ )	−3.513
13	Chemical Potential ( $\alpha$ )	−4.669

The dipole moment ( $\mu$ ) of an inhibitor gives an idea about the inhibitor's contact with the surface of a metal. Higher dipole moment always suggests an excellent interplay bearing high inhibition efficiency. The olmesartan molecule's dipole moment is about 7.83, which is very high compared with earlier results [28].

According to a literature review, a soft molecule is more reactive than a hard molecule, and the energy difference is proportional to the softness or hardness of the molecule [29,30]. According to our findings, olmesartan has a low energy gap and a significantly high dipole moment, suggesting that a reactive, soft molecule has corrosion inhibitor characteristics. Furthermore, higher molecular weight of an inhibitor, small energy gap, and low electronegativity increase its effective adsorption on steel surfaces, leading to a lower metal corrosion rate.

All of the above quantum chemical results suggest that the olmesartan molecule behaves as an excellent corrosion inhibitor. The quantum parameters give a preliminary idea of whether the molecule acts as a corrosion inhibitor, and they justify the experimental results.

**Figure 2.** The optimized molecular structure of olmesartan.

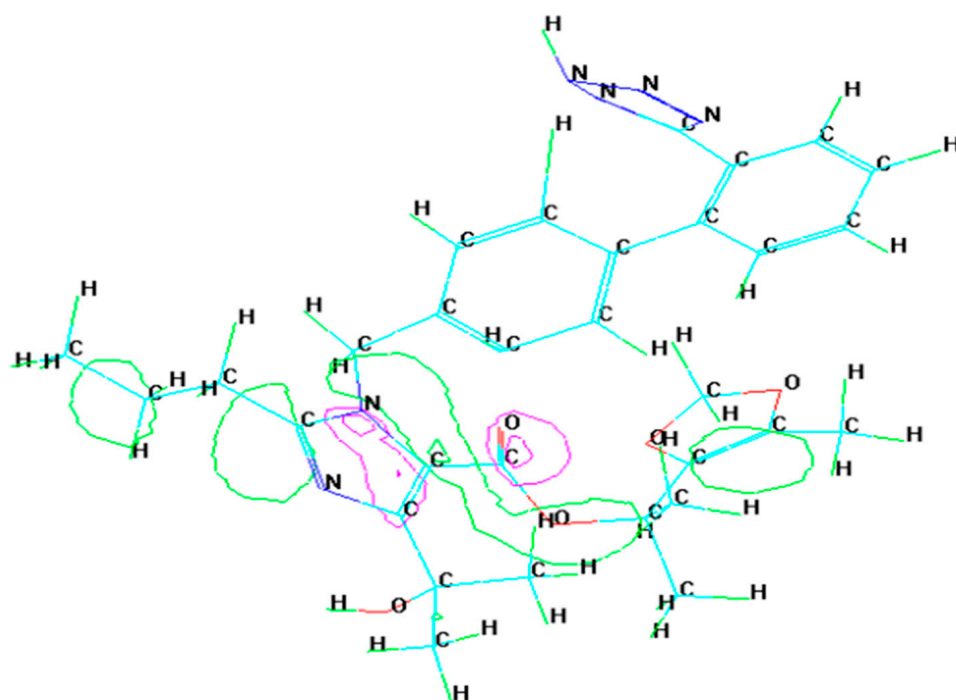


Figure 3. HOMO energy state of olmesartan.

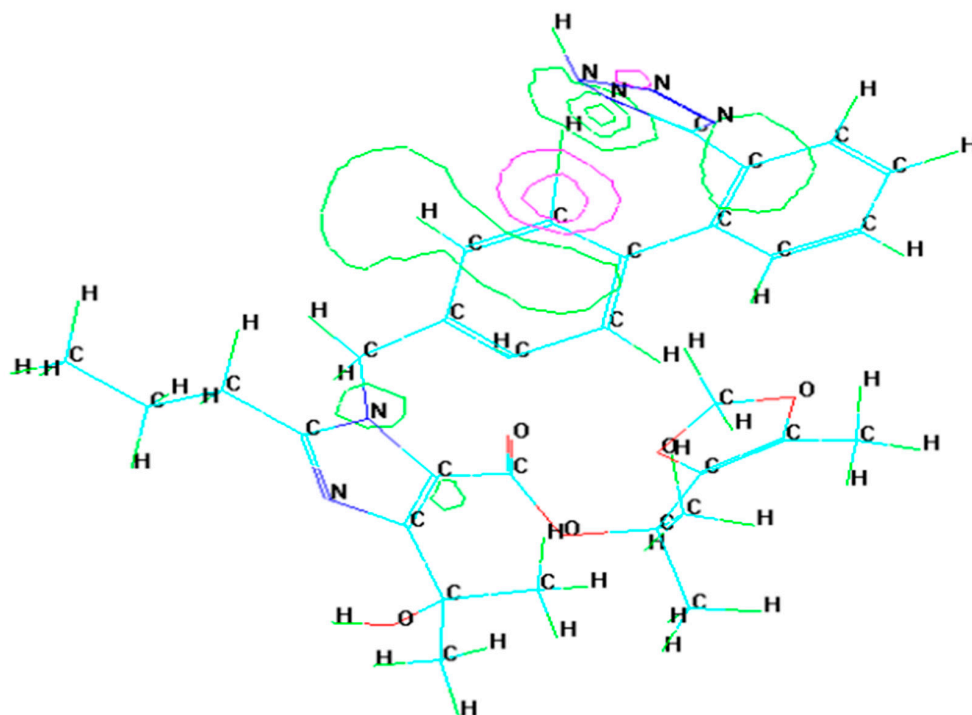


Figure 4. LUMO energy state of olmesartan.

### 3.2. Molecular Dynamics Simulation

The best approach for studying the adsorption interaction of an inhibitor with the metal surface is molecular dynamics (MD) simulations. The beginning of the simulation involves geometry optimization of inhibitors, solvent molecules ( $\text{H}_2\text{O}$ ), and corrosive ions ( $\text{H}_3\text{O}^+$ ). The simulation occurred when the temperature and energy of the system were



in equilibrium. Then, the  $E_{\text{interaction}}$  and  $E_{\text{binding}}$  energies of the adsorbed inhibitor on the surface were calculated using the following equations:

$$E_{\text{interaction}} = E_{\text{total}} - (E_{\text{surface}} + H_2O + H_3O^+ + Cl^- + E_{\text{inhibitor}}) \quad (7)$$

where the total energy of the simulation system is referred to as  $E_{\text{total}}$ .  $E_{\text{inhibitor}}$  energy of the free inhibitor molecule ( $E_{\text{surface}} + H_2O + H_3O^+ + Cl^-$ ) is equal to the energy of the iron surface with  $H_2O$ ,  $H_2O^+$ , and  $Cl^-$  ions, and the binding energy is given by

$$E_{\text{interaction}} = -E_{\text{binding}} \quad (8)$$

The absorption of an inhibitor molecule over the surface of Fe (110) is shown in Figures 5–7 and provides a strong adsorption situation. The observation that the inhibitor molecules adsorb on the iron layer suggests that chemical bonds between the inhibitor and the metal surface are developed. The shortest bond length for the inhibitor and Fe is  $2.9468 \text{ \AA}$ . This value means that there is a chemical bond created between the metal and the inhibitor. Hence, chemisorption occurs on the Fe surface. The interaction energy of the system is 16,575 kcal/mol. This considerable value indicates a more vital interaction between metal and inhibitor. These values also imply that inhibitor molecule adsorption takes place spontaneously. The higher the binding energy is another crucial factor in measuring the adsorption behavior. A higher binding energy value indicates that stronger adsorption is taking place between metal and inhibitor. These findings are in strong correlation with quantum parameters and are verified by practical effects.

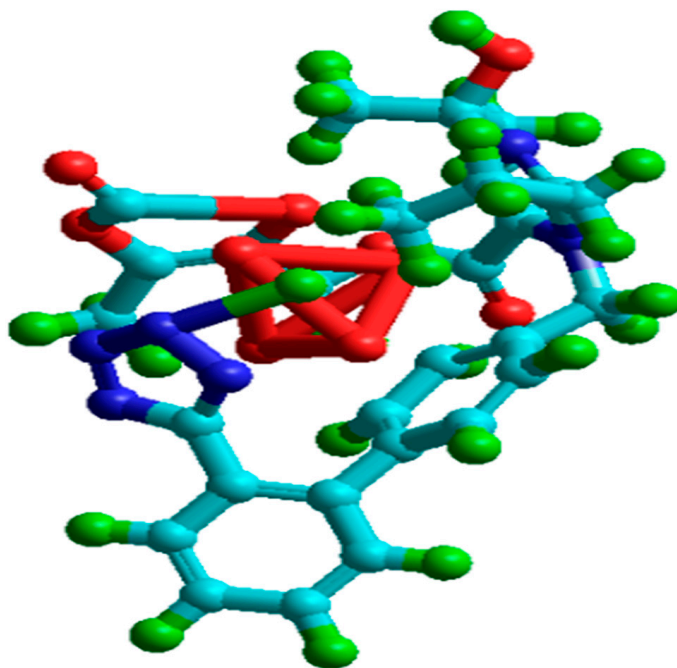


**Figure 5.** Interaction of Fe (110) with olmesartan molecule.

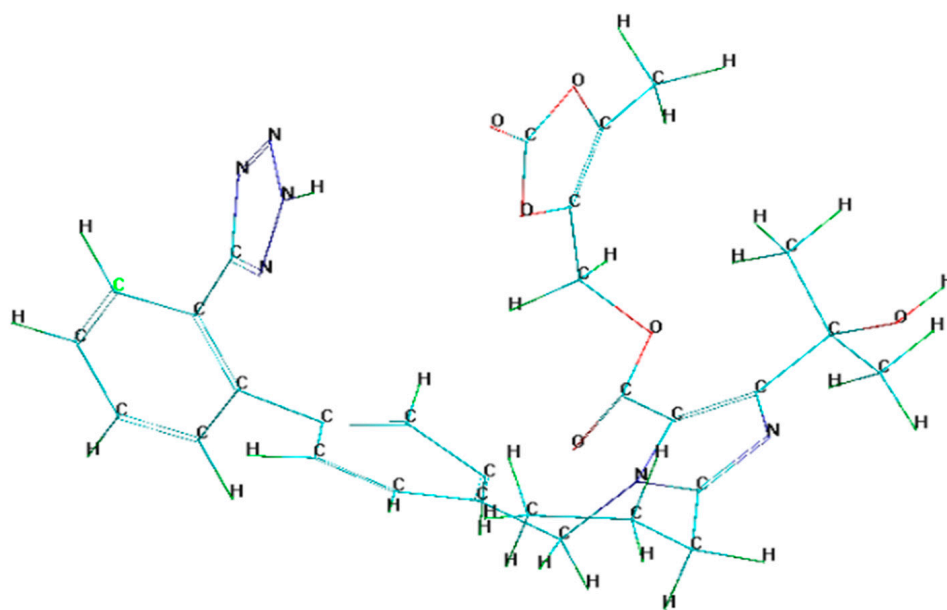


Figure 6. The optimized structure of olmesartan.

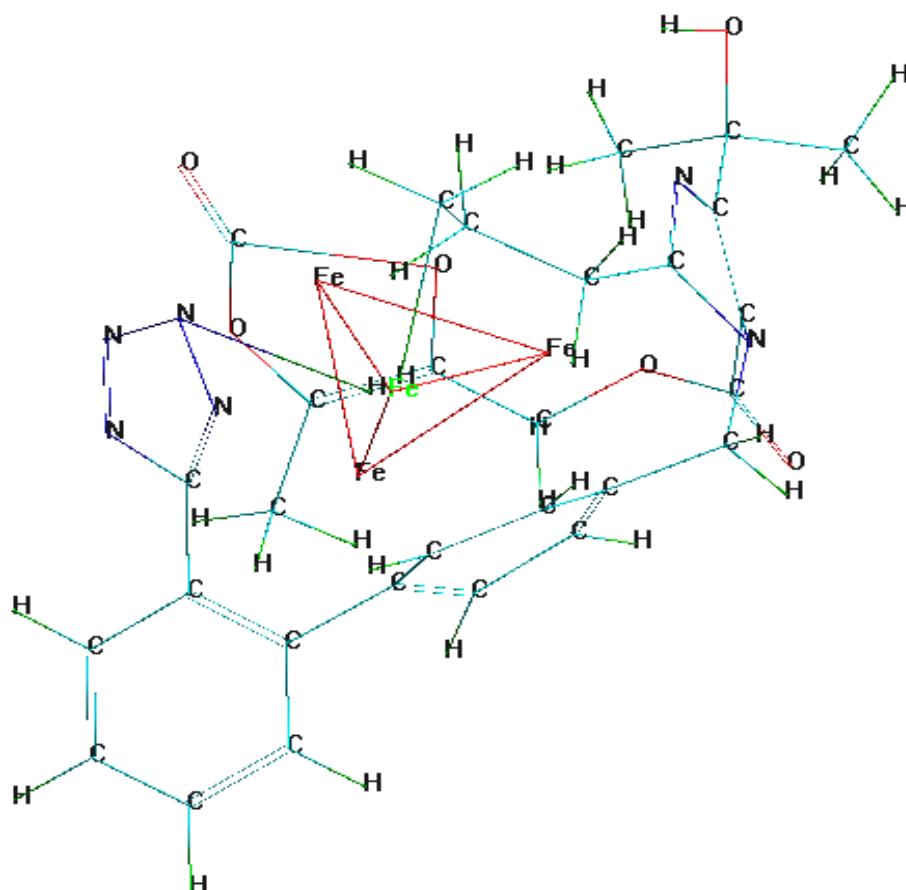


Figure 7. Interaction of  $\text{Fe}^{+4}$  with olmesartan molecular dynamics.

### 3.3. Potentiodynamic Polarization Measurements

The soft-cast steel was subjected to potentiodynamic polarization studies in  $1 \text{ mol dm}^{-3}$  HCl. Potentiodynamic polarization plots are also referred to as Tafel plots, which were recorded for soft-cast steel without and with the addition of various concentrations of



olmesartan in  $1 \text{ mol dm}^{-3}$  HCl at temperatures ranging from 303 K to 333 K, as described in Figure 8. Tafel plots were evaluated and discussed in contrast to corrosion kinetic parameters such as corrosion potential ( $E_{\text{corr}}$ ), corrosion current density ( $i_{\text{corr}}$ ), cathodic Tafel slope ( $C$ ), anodic Tafel slope ( $a$ ), and corrosion rate ( $v$ ). The following expression measures the inhibition efficiency ( $\eta_p$ ) of olmesartan for soft-cast steel in 1 M HCl:

$$\eta_p = \frac{i_0 - i}{i_0} \times 100 \quad (9)$$

where  $i_0$  and  $i$  are described as the corrosion current density for soft-cast steel without and with the addition of different concentrations of olmesartan in  $1 \text{ mol dm}^{-3}$  HCl. Table 3 shows the corrosion parameters calculated using the Tafel polarization method. The potentiodynamic polarization measurement for soft-cast steel without and with the addition of different concentrations of olmesartan in  $1 \text{ mol dm}^{-3}$  HCl indicates that the inhibition efficiency increases as the concentration is increased.

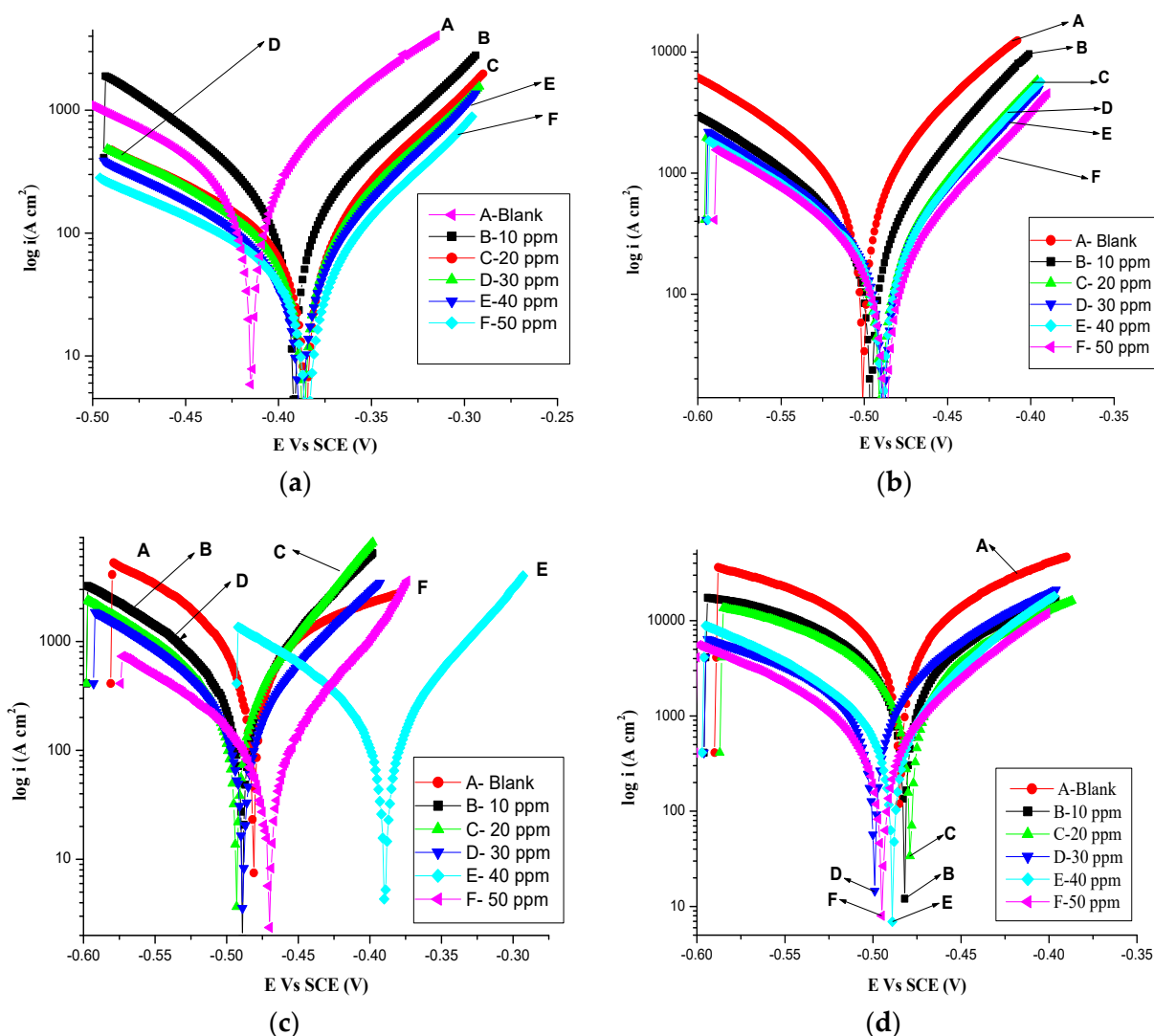


**Figure 8.** Soft cast steel Tafel polarization graphs without and with the various concentrations of olmesartan in  $1 \text{ mol dm}^{-3}$  HCl at elevated temperatures of (a) 303 K, (b) 313 K, (c) 323 K, and (d) 333 K.

**Table 3.** The corrosion parameters by potentiodynamic polarization measurement.

Temp (K)	Concentration of Olmesartan (ppm)	E <sub>corr</sub> (V)	i <sub>corr</sub> (μA cm <sup>-2</sup> )	v <sub>corr</sub> (mpy)	β <sub>c</sub> (mV/dec)	β <sub>a</sub> mV/dec	η <sub>p</sub> %
303	Blank	−0.415	0.228	0.369	−121	75	-
	10	−0.389	0.180	0.211	−84	74	21.05
	20	−0.388	0.100	0.121	−121	68	56.14
	30	−0.387	0.090	0.105	−111	70	60.52
	40	−0.386	0.084	0.082	−117	64	63.15
	50	−0.383	0.059	0.070	−135	67	69.29
313	Blank	−0.500	0.730	1.81	−102	70	-
	10	−0.495	0.297	0.481	−099	59	59.25
	20	−0.486	0.220	0.356	−109	62	69.81
	30	−0.486	0.211	0.341	−102	65	71.09
	40	−0.486	0.200	0.324	−106	61	72.50
	50	−0.484	0.172	0.278	−103	65	76.38
323	Blank	−0.481	0.733	8.514	−104	156	-
	10	−0.486	0.327	0.547	−66	105	55.33
	20	−0.489	0.250	0.415	−60	106	65.89
	30	−0.485	0.241	0.312	−71	102	67.12
	40	−0.386	0.230	0.248	−67	105	68.62
	50	−0.468	0.202	0.146	−65	109	72.44
333	Blank	−0.481	0.903	10.68	−129	96	-
	10	−0.472	0.495	4.776	−90	136	45.18
	20	−0.472	0.445	3.672	−128	92	50.71
	30	−0.502	0.402	2.074	−120	81	55.48
	40	−0.487	0.302	1.270	−96	61	66.55
	50	−0.491	0.281	0.908	−101	64	68.88

The determined inhibition efficiency for olmesartan of about 76.38% was observed at 50 ppm in concentration in 1 mol dm<sup>−3</sup> HCl at 313 K. Thus, the inhibition effect inhibitor was decreased as the temperature was increased up to 313 K. The increasing inhibition efficiency was due to inhibitor molecules' adsorption over soft-cast steel surfaces from the solution. The hydrogen liberation and metal dissolution are associated with the cathodic and anodic reactions, respectively, and both these responses are reduced in the presence of olmesartan.

A shift in the values of E<sub>corr</sub> for an inhibited solution concerning an uninhibited solution is around 32 mV, which is the indication that the olmesartan behaves as a mixed-type inhibitor in nature [31,32]. Hence, the overall inhibition effect is due to olmesartan adsorption blocking active corrosion sites on steel surfaces. The blocking of inhibitor molecules retards the electrochemical reaction, which reduces the corrosion of steel. The decreasing values of corrosion current densities indicate that the decrease of metal dissolution. The inhibitor inhibits both anodic and cathodic reactions, resulting in a decreased corrosion rate [33].

### 3.4. Electrochemical Impedance Spectroscopy (EIS) Measurement

EIS measurements were carried out on soft-cast steel without and with various concentrations of olmesartan in 1 mol dm<sup>−3</sup> HCl. Figure 9 shows the Nyquist plots for this study, and Figure 10 shows the EIS data fitted with an electrical equivalent circuit. Table 4 shows the corrosion parameters calculated for EIS measurements, for instance polarization resistance (R<sub>p</sub>) and double-layer capacitance (Cdl). The following equation is used to calculate the inhibition efficiency (η<sub>Z</sub>) of olmesartan,

$$\eta_Z = \frac{R_P - R_P^0}{R_P} \times 100 \quad (10)$$

where  $R_p$  and  $R_p^0$  are the polarization resistances of soft-cast steel without and with the addition of different concentrations of olmesartan in  $1 \text{ mol dm}^{-3}$  HCl, respectively.

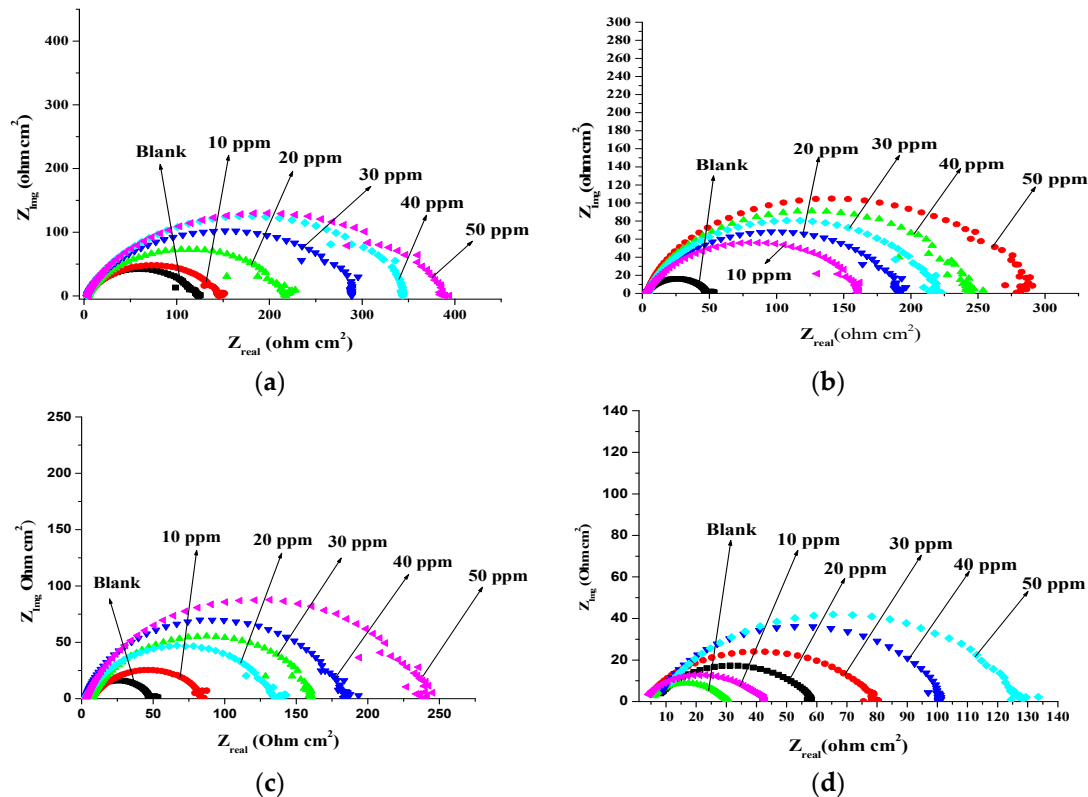


**Figure 9.** The Nyquist graphs of soft-cast steel without and with the various concentrations of olmesartan in  $1 \text{ mol dm}^{-3}$  HCl at temperatures of (a) 303 K, (b) 313 K, (c) 323 K, and (d) 333 K.

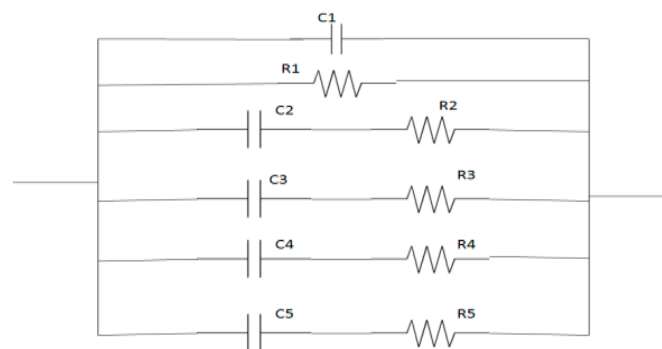


**Figure 10.** Electrically equivalent circuit to fit EIS data, where  $R_1$ ,  $R_2$ ,  $R_3$ ,  $R_4$ , and  $R_5$  are the resistances;  $C_1$ ,  $C_2$ ,  $C_3$ ,  $C_4$ , and  $C_5$  are the capacitances.

Because of frequency dispersion at the interfacial impedance of the metal surface caused by inhibitor molecule adsorption [34], Nyquist plots were obtained. Confirmation of the development of a protecting layer at the interface of the metal and the solution is indicated by decreasing  $C_{dl}$  values as the concentrations of inhibitor increased. Consequently, the decreasing values of  $C_{dl}$  are attributed to the adsorption of olmesartan to the metal surface by displacing the water molecules and other ions previously adsorbed on it. Additionally, decreasing  $C_{dl}$  values also indicate the increasing thickness of a double layer or the shielding of the metal surface by inhibitor molecule. The inhibitor molecules are chemically adsorbed onto the steel surface, forming a protective coating that inhibits corrosion [35]. The inhibition efficiency of olmesartan is increased due to providing a

protective layer at the metal/solution interface and the increasing concentration of the inhibitor in 1 mol dm<sup>−3</sup> HCl.

**Table 4.** The corrosion parameters for soft-cast steel in 1 mol dm<sup>−3</sup> HCl by EIS measurement.

Temp	Concentration of Olmesartan (ppm)	$R_p$ $\Omega$ cm <sup>2</sup>	$C_{dl}$ (F/cm <sup>2</sup> )	$\eta_z$ (%)	Surface Coverage $\theta$
303 K	Blank	120.7	0.032	-	-
	10	143.1	0.028	15.65	0.156
	20	212.9	0.026	43.30	0.433
	30	285.7	0.013	57.75	0.577
	40	340.0	0.010	64.50	0.645
	50	376.9	0.010	67.97	0.679
313 K	Blank	48.12	0.021	-	-
	10	158.00	0.014	69.54	0.695
	20	188.00	0.013	74.40	0.744
	30	215.00	0.010	77.61	0.776
	40	238.60	0.012	79.83	0.798
	50	281.80	0.009	82.92	0.829
323 K	Blank	48.12	0.024	-	-
	10	82.22	0.023	41.47	0.414
	20	132.80	0.020	63.76	0.637
	30	157.20	0.017	69.38	0.693
	40	196.50	0.015	75.51	0.755
	50	236.00	0.013	79.61	0.796
333 K	Blank	30.35	0.0321	-	-
	10	41.25	0.0315	40.51	0.405
	20	59.68	0.0305	49.14	0.491
	30	79.98	0.0236	62.05	0.620
	40	101.10	0.0226	70.75	0.707
	50	131.60	0.0212	76.93	0.769

The EIS provides a single depressed semicircle, and the semicircle's diameter increases as olmesartan increase its concentration. Therefore, the semi-circular appearance shows that the charge transfer regulates steel corrosion, and the inhibitor does not alter the metal dissolution process. The frequency dispersion of the interfacial impedance can determine the deviation of an arch from the circular shape [36]. It is also generally due to the metal surface's inhomogeneity due to the character of the surface roughness. Increasing  $R_p$  and decreasing  $C_{dl}$  values with an increasing concentration of inhibitor suggests forming a protective layer on the surface of the metal and preventing corrosion [37].

### 3.5. Thermodynamics

The adsorption of inhibitor molecules on metal surfaces reduces the corrosion rate of soft-cast steel. The inhibitor molecules from the bulk of the solution were observed blocking the active corrosion sites above the metal surfaces. The EIS parameters showed the mode of adsorption, such as the degrees of surface coverage ( $\theta$ ). We find a series of straight lines closer to unity with the linear regression coefficient ( $R^2$ ), which defines the adsorption isotherm model. As shown in Figure 11, the Temkin adsorption isothermal model was the best fit for the present study. The expression for the adsorption isotherm of the Temkin is

$$-2a\theta = \ln K_{ads} + \ln C \quad (11)$$

where  $C$  defines the solution concentration of olmesartan in terms of mol L<sup>−1</sup>,  $K_{ads}$  is the equilibrium constant for the adsorption process, which is associated with the following standard free energy change [38]:

$$K_{ads} = 1/55.5 \exp(\Delta G_{ads}^0 / RT) \quad (12)$$

where  $R$  is the universal ideal gas constant,  $T$  is the absolute temperature, and water concentration in solution ( $\text{mol}/\text{dm}^3$ ) is the standard value of 55.5.  $e K_{ad}$  values can be determined by the straight-line intercept obtained from the Temkin adsorption isotherm plot, and the calculated results are reported in Table 5.

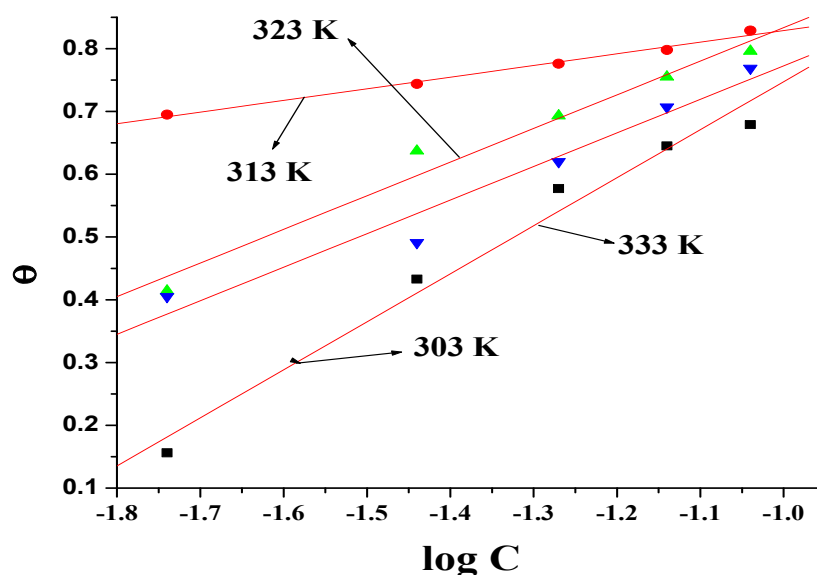


Figure 11. Temkin adsorption isotherm model.

Table 5. Thermodynamic data for steel surfaces in the absence and presence of various concentrations of olmesartan in  $1 \text{ mol dm}^{-3}$  HCl at temperatures ranging from 303 K to 333 K.

Temperature (K)	$K_{ads}$ (kJ/mol)	$\Delta G_{ads}^0$ (kJ/mol)
303	661.37	−26.47
313	986.19	−28.39
323	730.46	−28.49
333	765.11	−29.50

The negative sign in Table 5 suggests that the inhibitor adsorbs spontaneously from 1 M HCl on soft-cast steel surfaces. Therefore, the values measured within the range from  $-40$  to  $-20$  kJ/mol suggest that the olmesartan has adsorbed on the metal surface [39,40].

### 3.6. Activation Parameters

Using activation parameters, we investigate the effect of temperature on an inhibition efficiency of an inhibitor for metal surface in an aggressive corrosive media. Therefore, Arrhenius and transition theory explored the activation parameters. The apparent activation energy ( $E_a^*$ ) measured by Arrhenius equation for soft-cast steel in  $1 \text{ mol dm}^{-3}$  M HCl is [41].

$$\ln v_{corr} = \ln A - \frac{E_a^*}{RT} \quad (13)$$

where  $v_{corr}$  is the rate of corrosion and plots a graph of  $\ln v_{corr}$  versus  $1000/T$ , providing a straight line with the slope of  $-E_a^*/R$  and intercept of  $\ln A$ , as presented in Figure 12. The computed activation parameters are reported in Table 6.

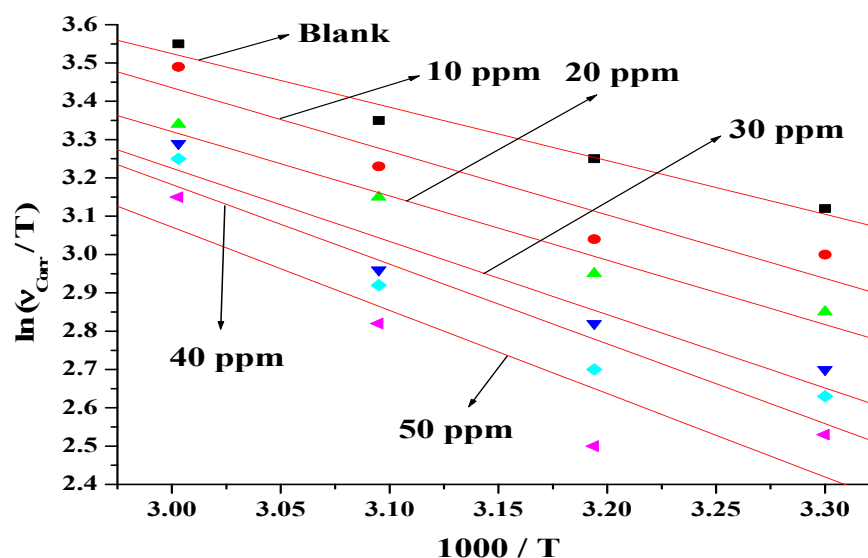


**Figure 12.** Arrhenius plot of soft-cast steel without and with the addition of various concentrations of olmesartan in  $1 \text{ mol dm}^{-3}$  of HCl at temperatures ranging from 303 K to 333 K.

**Table 6.** Activation parameters for steel surfaces in the absence and presence of various concentrations of olmesartan in  $1 \text{ mol dm}^{-3}$  HCl at temperatures ranging from 303 K to 333 K.

Concentration of Olmesartan (ppm)	$E_a^*$ (kJ/mol)	$A$ ( $\text{g/cm}^2/\text{h}$ )	$\Delta H^*$ (kJ/mol)	$\Delta S^*$ ( $\text{J/mol/K}^{-1}$ )
Blank	11.61	$22.46 \times 10^2$	9.09	−22.80
10	13.79	$45.05 \times 10^2$	11.27	−22.10
20	13.95	$42.59 \times 10^2$	11.44	−22.16
30	15.89	$78.00 \times 10^2$	13.11	−21.65
40	17.29	$123.82 \times 10^2$	14.44	−21.21
50	18.07	$146.76 \times 10^2$	15.48	−20.95

For inhibited solutions, the  $E_a^*$  values are greater than in an uninhibited solution that controls the corrosion rate for soft-cast steel. The increased apparent activation energy in the inhibited solution for the dissolution of carbon steel can be interpreted as physical adsorption. Since the inhibition efficiency of an inhibitor decreases with increasing temperature due to increased activation energy value, with increasing temperature, the inhibition efficiency of olmesartan decreases.

A transition theory equation, used to measure the enthalpy ( $\Delta H^*$ ) and entropy ( $\Delta S^*$ ) change in activation, is as follows:

$$\ln \frac{v_{corr}}{T} = \left[ \ln \frac{R}{Nh} + \frac{\Delta S^*}{R} \right] - \frac{\Delta H^*}{RT} \quad (14)$$

where  $N$  designates the Avogadro number and  $h$  represents the plank's constant. Plotting a graph of transition theory  $\ln(\frac{v_{corr}}{T})$  against  $1/T$  provides a set of straight lines with a slope value that describes the  $\Delta H^*$  value as shown in Figure 13. Computational values are listed in Table 6. Positive values of  $\Delta H^*$  indicate the endothermic nature of the steel dissolution phase. The shift in negative value from an increased concentration of olmesartan is the driving force to overcome its adsorption barriers on the steel surface.



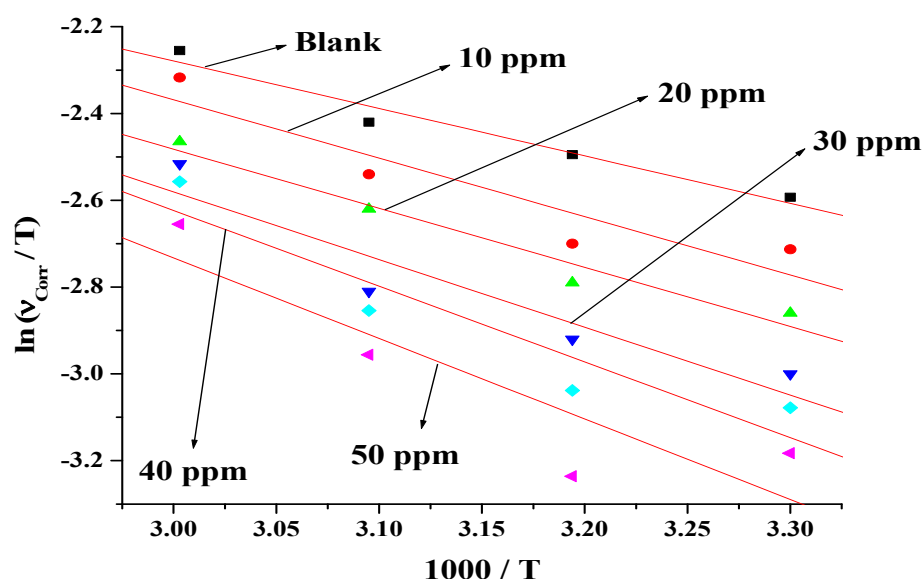
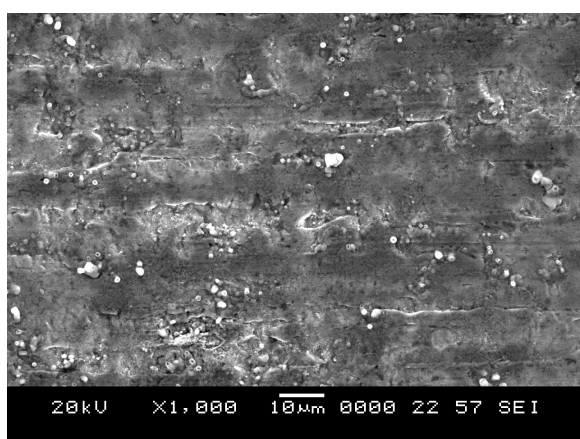


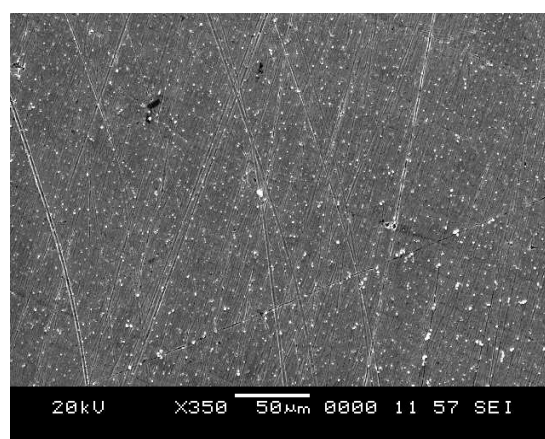
**Figure 13.** Transition state plot for soft-cast steel without and with the addition of different concentrations of olmesartan in  $1 \text{ mol dm}^{-3}$  HCl at temperatures ranging from 303 K to 333 K.

### 3.7. SEM Analysis

SEM is a familiar study of the surface characterization for soft-cast steel without and with the olmesartan concentration of about 50 ppm in  $1 \text{ mol dm}^{-3}$  M HCl. Figure 14 shows the SEM micrographs. Closely examining Figure 14A shows that a damaged surface is obtained when soft-cast steel is dipped in  $1 \text{ mol dm}^{-3}$  HCl solution in the absence of an inhibitor solution due to corrosion attack. However, the surface shows less corrosion and good smoothness in the presence of an inhibitor in Figure 14B. The inhibitor molecules provide a protective layer on the metal surface, decreasing corrosion of soft-cast steel [42].



(A)



(B)

**Figure 14.** SEM micrographs of soft-cast steel surface in (A)  $1 \text{ mol dm}^{-3}$  HCl (B) 50 ppm concentration of olmesartan in  $1 \text{ mol dm}^{-3}$  HCl.

## 4. Conclusions

An olmesartan drug was investigated as a corrosion inhibitor for soft-cast steel in  $1 \text{ mol dm}^{-3}$  HCl at temperatures ranging from 303 K to 333 K. Primarily, the anti-corrosion property of olmesartan molecule was investigated with quantum and molecular dynamics simulation studies helps to know the feasibility for this current research without any experiments. Theoretical measurements confirmed that the olmesartan molecule suitably

behaves as an effective corrosion inhibitor for soft-cast steel in 1 mol dm<sup>−3</sup> HCl. Therefore, the maximum inhibition efficiency of ~80% at 50 ppm was attained. The key points of this study are mentioned below.

- Quantum chemical parameters of olmesartan include a low energy gap value ( $\Delta E$ ) = 7.026 eV and high dipole moment value ( $\mu$ ) = 7.83, suggesting that the olmesartan serves as an effective corrosion inhibitor for soft-cast steel in 1 mol dm<sup>−3</sup> HCl.
- Molecular dynamic simulations anticipated spontaneous adsorption of olmesartan on the surface of soft-cast steel by involving C, N, and O elements. They also confirmed that the back-donation of electrons from the metal surface to the olmesartan molecule increases the stability of the inhibitor layer.
- Electrochemical measurements such as polarization and impedance spectroscopy suggest that an inhibitor's inhibition efficiency increases in its increasing concentrations in 1 mol dm<sup>−3</sup> HCl. The inhibitory activity of olmesartan is attributed to its adsorption onto the surface of soft-cast steel.
- Olmesartan adsorption obeyed Temkin's isotherm model with the values of  $\Delta G_{ads}^0$  within the −40 to −20 kJ/mol range suggesting a mixed-mode of physisorption and chemisorption.
- The activation parameters determine the effect of temperature on the inhibition efficiency of olmesartan in 1 mol dm<sup>−3</sup> HCl for soft-cast steel. The inhibition efficiency of olmesartan decreases with the increasing the temperature.
- The SEM images for soft-cast steel in the presence of olmesartan in 1 mol dm<sup>−3</sup> HCl, indicate the smooth and uniform adsorption process of the metal surface's protective barrier.

Olmesartan is an effective corrosion inhibitor for soft-cast steel in 1 mol dm<sup>−3</sup> HCl, considering the above theoretical and experimental considerations. Hence, it can be used in various reaction vessels and storage containers, which are having aggressive corrosive media. Additionally, this work can be extended for different metal surfaces to protect from corrosion attacks.

**Author Contributions:** Conceptualization, A.A. and B.M.P. (B. M. Praveen); methodology, B.M.P. (B. M. Praveen) and B.M.P. (B. M. Prasanna); software, A.A.; validation, N.H., B.M.P. (B. M. Prasanna), N.H., and A.A.; formal analysis, N.H. and A.A.; investigation, A.A.; resources, A.A.; writing—original draft preparation, B.M.P. (B. M. Prasanna); writing—review and editing, R.P., B.M.P. (B. M. Praveen). All authors have read and agreed to the published version of the manuscript.

**Funding:** This research was funded by Taif University Researchers Supporting Project No. (TURSP-2020/47), Taif University, Taif, Saudi Arabia.

**Institutional Review Board Statement:** Not Applicable.

**Informed Consent Statement:** Not Applicable.

**Data Availability Statement:** Data are included within the manuscript.

**Acknowledgments:** The authors would like to thank the Ministry of Education in Saudi Arabia and Taif University Researchers Supporting Project No. (TURSP-2020/47), Taif University, Taif, Saudi Arabia. Additionally, thanks to Srinivas University, Mangalore and Jain Institute of Technology, Davanagere, for their laboratory facility for this investigation.

**Conflicts of Interest:** The authors declare no conflict of interest.

## References

1. Zhang, Q.B.; Hua, Y.X. Corrosion inhibition of mild steel by alkyl imidazolium ionic liquids in hydrochloric acid. *Electrochem. Acta* **2009**, *54*, 1881. [\[CrossRef\]](#)
2. Quraishi, M.A.; Rawat, J. Inhibition of mild steel corrosion by some macrocyclic compounds in hot and concentrated hydrochloric acid. *Mater. Chem. Phys.* **2002**, *73*, 118. [\[CrossRef\]](#)
3. Banuprakash, G.; Prasanna, B.M.; Santhosh, B.M.; Guruprasad, A.M. Corrosion Inhibitive Capacity of Vanillin-Based Schiff Base for Steel in 1 M HCl. *J. Fail. Anal. Prev.* **2021**, *21*, 89–96. [\[CrossRef\]](#)

4. Lagrenee, M.; Bentiss, F.; Vezin, H.; Lagrenée, M. The inhibition of mild steel corrosion in acidic solutions by 2,5-bis(4-pyridyl)-1,3,4-thiadiazole: Structure-activity correlation. *Corros. Sci.* **2006**, *48*, 1279. [\[CrossRef\]](#)
5. Matad, P.B.; Mokshanatha, P.B.; Hebbar, N.; Venkatesha, V.T.; Tandon, H.C. Ketosulfone Drug as a Green Corrosion Inhibitor for Mild Steel in Acidic Medium. *Ind. Eng. Chem. Res.* **2014**, *53*, 8436. [\[CrossRef\]](#)
6. Guruprasad, A.M.; Sachin, H.P.; Swetha, G.A.; Prasanna, B.M. Corrosion inhibition of zinc in 0.1 M hydrochloric acid medium with clotrimazole: Experimental, theoretical and quantum studies. *Surf. Interfaces* **2020**, *19*, 100478. [\[CrossRef\]](#)
7. Swetha, G.A.; Sachin, H.P.; Guruprasad, A.M.; Prasanna, B.M. Rizatriptan Benzoate as Corrosion Inhibitor for Mild Steel in Acidic Corrosive Medium: Experimental and Theoretical Analysis. *J. Fail. Anal. Prev.* **2019**, *19*, 1113. [\[CrossRef\]](#)
8. Hebbar, N.; Praveen, B.M.; Prasanna, B.M.; Deepa, A. Electrochemical and Adsorption Studies of Telmisartan for Mild Steel in Acidic Medium. *J. Bio Tribo Corros.* **2019**, *5*, 40. [\[CrossRef\]](#)
9. Guruprasad, A.M.; Sachin, H.P.; Swetha, G.A.; Prasanna, B.M. Adsorption and inhibitive properties of Seroquel drug for zinc corrosion in 0.1 M hydrochloric acid solution. *Int. J. Ind. Chem.* **2019**, *10*, 17. [\[CrossRef\]](#)
10. Prasanna, B.M.; Praveen, B.M.; Hebbar, N.; Pavitra, M.K.; Manjunatha, T.S.; Malladi, R.S. Theoretical and experimental approach of inhibition effect by sulfamethoxazole on mild steel corrosion in 1-M HCl. *Surf. Interface Anal.* **2018**, *50*, 779. [\[CrossRef\]](#)
11. Praveen, B.M.; Prasanna, B.M.; Hebbar, N.; Kumar, P.S.; Jagadeesh, M.R. Experimental and Theoretical Studies on Inhibition Effect of the Praziquantel on Mild Steel Corrosion in 1 M HCl. *J. Bio Tribo Corros.* **2018**, *4*, 21. [\[CrossRef\]](#)
12. Hebbar, N.; Praveen, B.M.; Prasanna, B.M.; Venkatarangiah, V.T.; Abd Hamid, S.B. Adsorption, thermodynamic, and electrochemical studies of Ketosulfide for mild steel in acidic medium. *J. Adhes. Sci. Technol.* **2015**, *29*, 2692. [\[CrossRef\]](#)
13. Prasanna, B.M.; Praveen, B.M.; Hebbar, N.; Venkatesha, T.V.; Tandon, H.C.; Abd Hamid, S.B. Electrochemical study on the inhibitory effect of Aspirin on mild steel in 1M hydrochloric acid. *J. Assoc. Arab. Univ. Basic Appl. Sci.* **2017**, *22*, 62. [\[CrossRef\]](#)
14. Hebbar, N.; Praveen, B.M.; Prasanna, B.M.; Venkatesha, T.V.; Abd Hamid, S.B. Anthranilic Acid as Corrosion Inhibitor for Mild Steel in Hydrochloric Acid Media. *Procedia Mater. Sci.* **2014**, *5*, 712. [\[CrossRef\]](#)
15. Praveen, B.M.; Prasanna, B.M.; Mallikarjuna, N.M.; Jagadeesh, M.R.; Hebbar, N.; Rashmi, D. Investigation of anticorrosive behaviour of novel tert-butyl 4-[(4-methyl phenyl) carbonyl] piperazine-1-carboxylate for carbon steel in 1M HCl. *Heliyon* **2021**, *7*, e06090. [\[CrossRef\]](#) [\[PubMed\]](#)
16. Mallikarjuna, N.M.; Keshavayya, J.; Prasanna, B.M.; Praveen, B.M.; Tandon, H.C. Synthesis, Characterization, and Anti-Corrosion Behavior of Novel Mono Azo Dyes Derived from 4,5,6,7-Tetrahydro-1,3-benzothiazole for Mild Steel in Acid Solution. *J. Bio Tribo Corros.* **2020**, *6*, 9. [\[CrossRef\]](#)
17. Padmashree, B.; Manjunatha, K.; Prasanna, B.M. Electrochemical Behavior of 1,3-bis(1-Phenylethyl) Urea as a Corrosion Inhibitor for Carbon Steel in 1 M HCl. *J. Fail. Anal. Prev.* **2020**, *20*, 226–234. [\[CrossRef\]](#)
18. Rajendraprasad, S.; Ali, S.; Prasanna, B.M. Electrochemical Behavior of N1-(3-Methylphenyl) Piperidine-1,4-Dicarboxamide as a Corrosion Inhibitor for Soft-Cast Steel Carbon Steel in 1 M HCl. *J. Fail. Anal. Prev.* **2020**, *20*, 235. [\[CrossRef\]](#)
19. Narayana, H.; Praveen, B.M.; Prasanna, B.M.; Vishwanath, P. Electrochemical and adsorption studies of 4-Chloro, 8-(Trifluoromethyl) Quinoline (CTQ) for mild steel in acidic media. *J. Fail. Anal. Prev.* **2020**, *20*, 1516–1523. [\[CrossRef\]](#)
20. Haris, N.I.N.; Sobri, S.; Yusof, Y.A.; Kassim, N.K. An Overview of Molecular Dynamic Simulation for Corrosion Inhibition of Ferrous Metals. *Metals* **2021**, *11*, 46. [\[CrossRef\]](#)
21. Maricica, S.; Lina, M.; Almira, R.; Petru, A.; Geta, C.; Rodica, D.; Jaroslav, V.; Arūnas, R. Corrosion Study of Stainless Steel Incubated in Solutions Consisting of Biocide (Oxonia-Active) and Aspergillus niger Suspension. *Chemija* **2012**, *23*, 180.
22. Hu, Y.; Xin, L.; Liu, T.; Lu, Y. Corrosion Behavior of L245N Standard Steel in CO<sub>2</sub> Saturated Brine under Flow Condition. *Metals* **2021**, *11*, 880. [\[CrossRef\]](#)
23. Mu, G.N.; Li, X.; Li, F. Synergistic inhibition between o-phenanthroline and chloride ion on cold-rolled steel corrosion in phosphoric acid. *Mater. Chem. Phys.* **2004**, *86*, 59. [\[CrossRef\]](#)
24. Ji, G.; Shukla, S.K.; Dwivedi, P.; Sundaram, S.; Prakash, R. Inhibitive Effect of Argemone mexicana Plant Extract on Acid Corrosion of Mild Steel. *Ind. Eng. Chem. Res.* **2011**, *50*, 11954–11959. [\[CrossRef\]](#)
25. Yadav, M.; Behera, D.; Kumar, S.; Sinha, R.R. Studied corrosion inhibition performance of three Benzimidazole derivatives for mild steel in HCl. *Ind. Eng. Chem. Res.* **2013**, *52*, 6318. [\[CrossRef\]](#)
26. Zhang, J.; Gong, X.L.; Yu, H.H.; Du, M. The inhibition mechanism of imidazoline phosphate inhibitor for Q235 steel in hydrochloric acid medium. *Corros. Sci.* **2011**, *53*, 3324. [\[CrossRef\]](#)
27. Nataraja, S.E.; Venkatesha, T.V.; Manjunatha, K.; Poojary, B.; Pavithra, M.K.; Tandon, H.C. Inhibition of the corrosion of steel in hydrochloric acid solution by some organic molecules containing the methylthiophenyl moiety. *Corros. Sci.* **2011**, *58*, 2651–2659. [\[CrossRef\]](#)
28. Badiea, A.M.; Mohana, K.N. Effect of temperature and fluid velocity on corrosion mechanism of low carbon steel in the presence of 2-hydrazino-4,7-dimethylbenzothiazole in industrial water medium. *Corros. Sci.* **2009**, *51*, 2231. [\[CrossRef\]](#)
29. Hebbar, N.; Praveen, B.M.; Prasanna, B.M.; Sachin, H.P. Anticorrosion Potential of Flectoferine on Mild Steel in Hydrochloric Acid Media: Experimental and Theoretical Study. *J. Fail. Anal. Prev.* **2018**, *18*, 371. [\[CrossRef\]](#)
30. Firdhouse, M.J.; Nalini, D. Corrosion Inhibition of Mild Steel in Acidic Media by 5'-Phenyl-2',4'-dihydrospiro[indole-3,3'-pyrazol]-2(1H)-one. *J. Chem.* **2013**, *2013*, 1. [\[CrossRef\]](#)
31. Laarej, K.; Bouachrine, M.; Radi, S.; Kertit, S.; Hammouti, B.E. Quantum Chemical Studies on the Inhibiting Effect of Bipyrazoles on Steel Corrosion in HCl. *J. Chem.* **2010**, *7*, 419. [\[CrossRef\]](#)

32. Ali, S.A.; El-Shareef, A.M.; Al-Ghandi, R.F.; Saeed, M.T. Synthesis of aza-pseudo peptides and the evaluation of their inhibiting efficacy of mild steel corrosion in 1.0 M HCl. *Corros. Sci.* **2005**, *47*, 2659. [[CrossRef](#)]
33. Jayaperumal, D. Effects of alcohol-based inhibitors on corrosion of mild steel in hydrochloric acid. *Mater. Chem. Phys.* **2010**, *119*, 478. [[CrossRef](#)]
34. Prasanna, B.M.; Praveen, B.M.; Hebbar, N.; Venkatesha, T.V.; Tandon, H.C. Inhibition study of mild steel corrosion in 1 M hydrochloric acid solution by 2-chloro 3-formyl quinoline. *Int. J. Ind. Chem.* **2016**, *7*, 9. [[CrossRef](#)]
35. Ahmad, I.; Prasad, R.; Quraishi, M.A. Adsorption and inhibitive properties of some new Mannich bases of Isatin derivatives on corrosion of mild steel in acidic media. *Corros. Sci.* **2010**, *52*, 1472. [[CrossRef](#)]
36. Zhao, J.; Chen, G. The synergistic inhibition effect of oleic-based imidazoline and sodium benzoate on mild steel corrosion in a CO<sub>2</sub>-saturated brine solution. *Electrochim. Acta* **2012**, *69*, 247. [[CrossRef](#)]
37. Swetha, G.A.; Sachin, H.P.; Guruprasad, A.M.; Prasanna, B.M.; Sudheer Kumar, K.H. Use of Seroquel as an Effective Corrosion Inhibitor for Low Carbon Steel in 1 M HCl. *J. Bio Tribo Corros.* **2018**, *4*, 57. [[CrossRef](#)]
38. Banuprakash, G.; Prasanna, B.M.; Hebbar, N.; Manjunatha, T.S. Inhibitive Capability of a Novel Schiff Base for Steel in 1 M HCl Media. *J. Fail. Anal. Prev.* **2020**, *20*, 572–579. [[CrossRef](#)]
39. Umoren, S.A.; Ogbobe, O.; Igwe, I.O.; Ebenso, E.E. Inhibition of mild steel corrosion in acidic medium using synthetic and naturally occurring polymers and synergistic halide additives. *Corros. Sci.* **2008**, *50*, 1998. [[CrossRef](#)]
40. Badiea, A.M.; Mohana, M.N. Novel cationic surfactants from fatty acids and their corrosion inhibition efficiency for carbon steel pipelines in 1 M HCl. *Corros. Sci.* **2009**, *51*, 2231. [[CrossRef](#)]
41. Ghasemi1, O.; Danaee1, I.; Rashed, G.R.; RashvandAvei, M.; Maddahy, M.H. Inhibition effect of a synthesized N, N'-bis(2-hydroxybenzaldehyde)-1,3-propandiimine on corrosion of mild steel in HCl. *J. Cent. South Univ.* **2013**, *20*, 301–311. [[CrossRef](#)]
42. Fouda, A.S.; Heakal, F.E.; Radwan, M.S. Role of some thiadiazole derivatives as inhibitors for the corrosion of C-steel in 1 M H<sub>2</sub>SO<sub>4</sub>. *J. Appl. Electrochem.* **2009**, *39*, 391. [[CrossRef](#)]